

Global description of the ${}^7\text{Li} + p$ reaction at 5.44 MeV/u in a continuum-discretized coupled-channels approach

A. Pakou,^{1,*} F. Cappuzzello,^{2,3} N. Keeley,⁴ L. Acosta,^{5,6} C. Agodi,² X. Aslanoglou,¹ S. Calabrese,^{2,3} D. Carbone,² M. Cavallaro,² A. Foti,^{3,6} G. Marquínez-Durán,⁷ I. Martel,⁷ M. Mazzocco,^{8,9} C. Parascandolo,¹⁰ D. Pierroutsakou,¹⁰ K. Rusek,¹¹ O. Sgouros,¹ V. Soukeras,¹ E. Strano,^{8,9} V. A. B. Zagatto,¹² and K. Zerva¹

¹*Department of Physics and HINP, The University of Ioannina, 45110 Ioannina, Greece*

²*INFN-Laboratori Nazionali del Sud, via Santa Sofia 62, 95125 Catania, Italy*

³*Dipartimento di Fisica e Astronomia, Università di Catania, via Santa Sofia 64, 95125 Catania, Italy*

⁴*National Centre for Nuclear Research, ulica Andrzeja Sołtana 7, 05-400 Otwock, Poland*

⁵*Instituto de Física, Universidad Nacional Autónoma de México, México Distrito Federal 01000, México*

⁶*INFN-Sezione di Catania, via Santa Sofia 64, 95125 Catania, Italy*

⁷*Departamento de Ciencias Integradas, Facultad de Ciencias Experimentales, Campus de El Carmen, Universidad de Huelva, 21071 Huelva, Spain*

⁸*Departamento di Fisica e Astronomia, Università di Padova, via Marzolo 8, I-35131 Padova, Italy*

⁹*INFN-Sezione di Padova, via Marzolo 8, I-35131 Padova, Italy*

¹⁰*INFN-Sezione di Napoli, via Cinthia, I-80126 Napoli, Italy*

¹¹*Heavy Ion Laboratory, University of Warsaw, ulica Pasteura 5a, 02-093 Warsaw, Poland*

¹²*Instituto de Física da Universidade Federal Fluminense, Avenida General Milton Tavares de Souza, Niterói, Brazil*

(Received 11 June 2017; revised manuscript received 22 August 2017; published 21 September 2017)

The complete set of open channels for the ${}^7\text{Li} + p$ system, namely elastic scattering, inelastic scattering, breakup, the ${}^7\text{Li} + p \rightarrow {}^7\text{Be} + n$ charge exchange reaction, and the ${}^7\text{Li} + p \rightarrow {}^4\text{He} + {}^4\text{He}$ reaction, was measured in the same experiment in inverse kinematics at an energy of 5.44 MeV/u. Data were also obtained for the charge exchange reaction at energies of 5.0 and 3.57 MeV/u. The elastic and inelastic scattering and breakup data were reported previously and are reviewed here and, together with the new data for the other two reactions, are discussed coherently within the same continuum-discretized coupled-channels model framework.

DOI: [10.1103/PhysRevC.96.034615](https://doi.org/10.1103/PhysRevC.96.034615)

I. INTRODUCTION

As part of an extensive program investigating proton scattering from weakly bound nuclei in inverse kinematics we recently considered the ${}^7\text{Li} + p$ elastic scattering at several near-barrier energies (2.29, 3.57, 5.0, and 5.44 MeV/u [1]). The measurements were performed using the MAGNEX spectrometer [2] of the Istituto Nazionale di Fisica Nucleare Laboratori Nazionali del Sud (INFN LNS) and the data were analyzed within the continuum-discretized coupled-channels (CDCC) approach. However, for a more effective interpretation of the experimental data in a channel coupling scheme a global investigation of all the reaction channels involved is necessary. In this spirit, we consider in this article simultaneous measurements of all open channels involved in the ${}^7\text{Li} + p$ reaction at 5.44 MeV/u ($E/V_C \sim 7$), that is, elastic scattering, inelastic scattering, breakup, the charge exchange reaction ${}^7\text{Li} + p \rightarrow {}^7\text{Be} + n$ to the ground and first excited states of ${}^7\text{Be}$, and the transfer/compound nucleus reaction ${}^7\text{Li} + p \rightarrow {}^4\text{He} + {}^4\text{He}$, all on the same footing. Data for the charge exchange reactions at 5.0 and 3.57 MeV/u are also presented. The elastic and inelastic scattering and breakup reaction channels were reported previously [1,3].

The effect of the breakup coupling on the elastic scattering is investigated in more detail and the new data for the

charge exchange and the (p,α) reactions are compared with previous measurements [4–6]. As the output of our CDCC calculations includes not only elastic, inelastic, and breakup angular distributions but also a total absorption cross section, these two reactions enable us further to test our CDCC calculations since the absorption cross section of the CDCC calculations should be equal to the sum of the measured charge exchange and (p,α) reactions, these being the only two open channels in this energy regime not explicitly included in the coupling scheme. Since the new complete data set at 5.44 MeV/u reported here was taken simultaneously in the same experiment, the absolute normalization of the individual channels is well established. The good agreement with the existing data for the charge exchange and (p,α) reactions where the two sets of measurement overlap therefore enables us to compare these data with our CDCC calculations at 5.0, 3.57, and 2.29 MeV/u where complete data sets were not obtained in a single experiment.

II. EXPERIMENTAL DETAILS

The experiment was performed at the INFN LNS in Catania, Italy, with data taken at incident ${}^7\text{Li}$ beam energies of 16, 25, 35, and 38.1 MeV. A description of the experimental setup may be found in Refs. [1,3] and only details pertinent to this work are given here. Simultaneously with the elastic and inelastic scattering reported in Ref. [1] data were collected for ${}^7\text{Be}$ (ground and first excited states) originating from the

*apakou@cc.uoi.gr

${}^7\text{Li} + p \rightarrow {}^7\text{Be} + n$ charge exchange reaction. During the exclusive breakup measurement performed at 38.1 MeV [3] a telescope from the GLORIA array [7], installed at 32.9° and subtending an angular range of 25° to 40.8° , was used to detect α particles originating from the transfer/compound nucleus reaction ${}^7\text{Li} + p \rightarrow {}^4\text{He} + {}^4\text{He}$. The chosen conditions allowed the detection of one of the two α particles over an angular range corresponding to $\theta_{\text{c.m.}} \sim 50^\circ$ to 90° in the center-of-mass frame. The normalization of the data was obtained taking into account the beam flux, derived from the charge collected by a Faraday cup set at the entrance of MAGNEX. The absolute value was cross checked via the elastic scattering measurements at the most forward angles where the scattering was dominated by the Rutherford mechanism. Therefore, since the whole of our data set was collected in the same experiment both the relative normalizations and the overall absolute normalization of the different channels could be accurately fixed, thus enabling us to validate the absolute normalizations of existing data from the literature for some of these reactions, obtained at different times by different groups. In this way data from different sources may be used together with confidence. Details of the data reduction procedures for the charge exchange and ${}^7\text{Li} + p \rightarrow {}^4\text{He} + {}^4\text{He}$ reactions are given in the following two sections.

A. The ${}^7\text{Li} + p \rightarrow {}^7\text{Be} + n$ reaction

The charge exchange reaction was studied in the same way as the elastic scattering, by detecting in MAGNEX the heavy ejectile, ${}^7\text{Be}$. Data populating both the ground and first excited states of ${}^7\text{Be}$ were analyzed and the corresponding counts in steps of 0.5° in the angular range from 0 to 10° deduced. Cross sections were extracted taking into account the same beam flux and solid angle as for the elastic scattering. Our angular distribution results for the ground and excited states are shown in Figs. 1 and 2, respectively, transformed to the center-of-mass system. The uncertainties were obtained by taking into account a 5% error in the beam flux, target scattering centers, and solid angle and a statistical error ranging from between 8% and 11% for the ground state and between 10% and 15% for the first excited state of ${}^7\text{Be}$. The results are compared with existing data at similar energies taken from Refs. [4,5] and are found to be in good agreement. Taking into account that the absolute normalization of the present data was checked against Rutherford scattering, the good agreement with the previous data allows us to use them with complete confidence together with the new data. Reaction cross sections at 5.44 MeV/u (38.1 MeV) were obtained by integrating the combined angular distributions and are listed in Table II.

B. The ${}^7\text{Li} + p \rightarrow {}^4\text{He} + {}^4\text{He}$ reaction

The ${}^7\text{Li} + p \rightarrow {}^4\text{He} + {}^4\text{He}$ reaction was studied simultaneously with the breakup. In this case the reaction products were not detected by MAGNEX but by a telescope of the GLORIA array, specifically installed in the reaction chamber for this purpose. The telescope comprised two detectors, a $50\text{-}\mu\text{m}$ -thick double-sided silicon strip detector

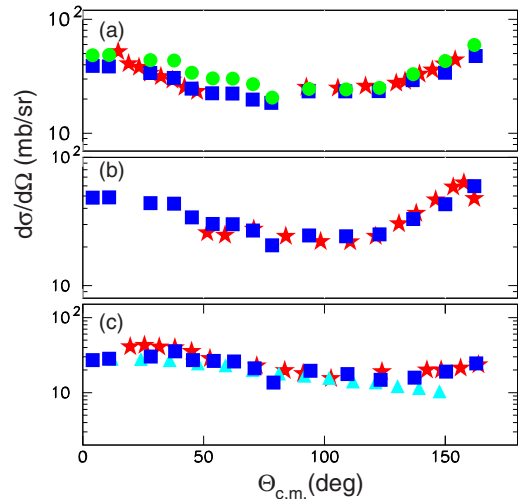


FIG. 1. The present experimental angular distributions for the ${}^7\text{Li} + p \rightarrow {}^7\text{Be} + n$ charge exchange reaction to the ${}^7\text{Be}$ ground state at (a) 5.44 MeV/u (38.1 MeV), (b) 5.0 MeV/u (35 MeV), and (c) 3.57 MeV/u (25 MeV) compared with existing data [4,5]. The present data are denoted by red stars while those from Ref. [4] are denoted by blue squares and refer to energies of (a) 5.5 MeV/u, (b) 5.0 MeV/u, and (c) 4.25 MeV/u and denoted by green circles in panel (a) and refer to an energy of 5.0 MeV/u. Data from Ref. [5] are denoted by cyan triangles in panel (c) and refer to an energy of 3.8 MeV/u. The uncertainties in the present data do not exceed 11% and are smaller than the size of the points.

(DSSSD) backed by a $1000\text{-}\mu\text{m}$ -thick silicon pad as the second stage. This telescope covered the angular range from 25° to 40.8° and allowed the detection of one α particle at energies corresponding to the first solution of the double-valued kinematical equation. The α particles from the second kinematical solution were not detected due to their very low energy. A two-dimensional plot is given in Fig. 3, and it can be seen that α particles are well discriminated from other light particles via the ΔE - E technique. In this two-dimensional plot the continuous α curve corresponds to evaporated α particles from a possible compound and/or breakup process of ${}^7\text{Li}$ on the carbon scattering centers in the CH_2 target. The α particles from the two-body reaction under consideration are denoted in the figure by the red (gray oval-shaped) spot. Counts were integrated for every strip of the DSSSD detector, taking into account graphical cuts around the red (gray oval-shaped) spot in the two-dimensional plots. These counts were normalized to the beam flux, obtained from the beam charge collected in a Faraday cup, the solid angle of the strips determined in a separate run with a gold target, and the scattering centers of the target.

The angular distribution obtained, transformed into the center-of-mass system, is shown in Fig. 4. The uncertainties do not exceed 8% of the cross section itself and are mainly due to uncertainties in the beam flux (5%), the scattering centers (5%), and the solid angle (4%), as the statistical error was less than 2%. Direct comparison of the normalization of the current angular distribution at 5.44 MeV/u with the measurements of Ref. [6] is complicated by the presence of a broad ${}^8\text{Be}$

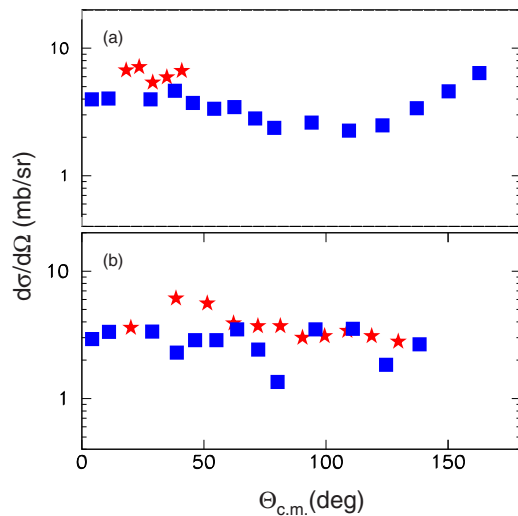


FIG. 2. The present experimental angular distributions for the ${}^7\text{Li} + p \rightarrow {}^7\text{Be}^* + n$ charge exchange reaction to the first excited state of ${}^7\text{Be}$ (red stars) at (a) 5.44 MeV/u (38.1 MeV) and (b) 3.57 MeV/u (25 MeV) compared with existing data [4] (blue squares) at (a) 5.5 MeV/u and (b) 4.2 MeV/u. The uncertainties in the present data do not exceed 15% and are smaller than the size of the points.

resonance at this energy range (see Fig. 11 of Ref. [6]) but the shape of the angular distribution is consistent with the previous measurement at 5.26 MeV/u. The current angular distribution was fitted with a sum of Legendre polynomials, as in Ref. [6], and the fit was integrated over angle to give a total cross section of 27 ± 3 mb, approximately 3/5 the value at the corresponding energy in the excitation function of Ref. [6].

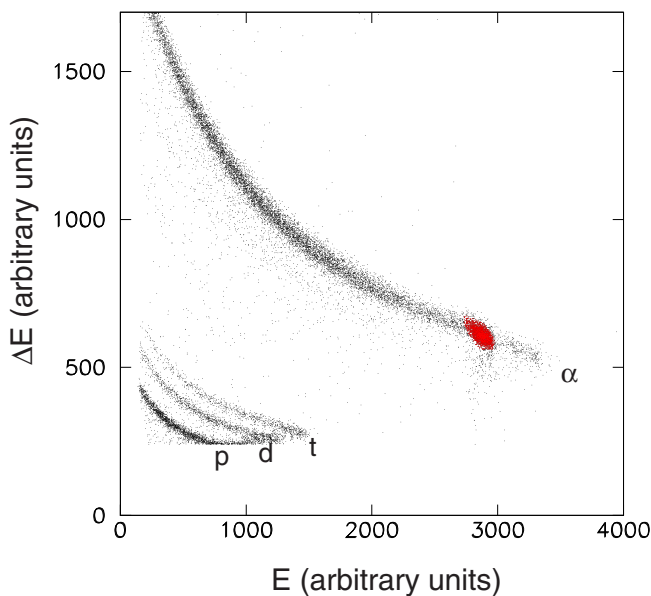


FIG. 3. Two-dimensional ΔE - E energy plot obtained for the ${}^7\text{Li} + p \rightarrow {}^4\text{He} + {}^4\text{He}$ reaction at 5.44 MeV/u (38.1 MeV) by one strip of the GLORIA DSSSD module ($\sim 40^\circ$).

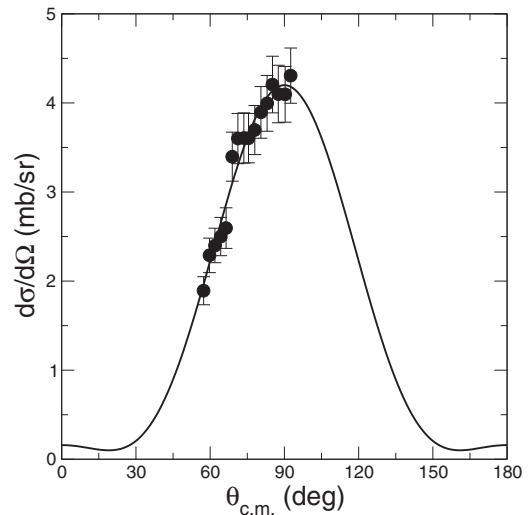


FIG. 4. Angular distribution for the ${}^7\text{Li} + p \rightarrow {}^4\text{He} + {}^4\text{He}$ reaction at 5.44 MeV/u. The present data are denoted by the solid circles. The solid curve denotes the Legendre polynomial fit to the angular distribution.

III. THE CDCC CALCULATIONS

The CDCC calculations adopting the $\alpha + t$ cluster model of ${}^7\text{Li}$ performed using the code FRESKO [8] were fully described in Refs. [1,3]. However, we take this opportunity to tabulate (Table I) the empirical $p + {}^4\text{He}$ and $p + t$ optical potentials, obtained by fitting existing $p + \alpha$ [9–11] and $p + t$ [12] elastic scattering data at the appropriate energies, used to obtain the ${}^7\text{Li} + p$ diagonal and coupling potentials via the Watanabe single-folding method. These calculations were able to describe well the elastic scattering, inelastic scattering, and ${}^7\text{Li} \rightarrow \alpha + t$ breakup (see Refs. [1,3]). Before passing to the new data for the charge exchange and ${}^7\text{Li}(p, {}^4\text{He}){}^4\text{He}$ reactions and their relevance in the context of the CDCC calculations, we make a few more detailed observations concerning the elastic and inelastic scattering and the breakup coupling effects.

It should be noted that the choice of projectile energies allows the influence of the cluster structure of the projectile as well as the couplings to the continuum to be probed step-by-step. At the lowest energy of 16 MeV (2.29 MeV/u) the available energy, $E_{\text{avail}} = 2.0 - 2.467 = -0.467$ MeV, does not permit excitation of the ${}^7\text{Li}$ to the continuum; therefore the cluster structure of the projectile is the only significant point in the calculation. At 25 MeV (3.57 MeV/u) the available energy, $E_{\text{avail}} = 3.125 - 2.467 = 0.658$ MeV, is just enough to enable excitation to the continuum, while at 35 MeV (5 MeV/u), $E_{\text{avail}} = 4.375 - 2.467 = 1.908$ MeV excitations to the low-lying continuum are established. Finally, at 38.1 MeV (5.44 MeV/u) $E_{\text{avail}} = 4.76 - 2.467 = 2.283$ MeV and excitations to direct and sequential breakup are both possible and their effect on the elastic scattering could be tested.

While we concentrate here on the data at 38.1 MeV (5.44 MeV/u), where all the open channels were measured, for the sake of completeness we compile the complete set of elastic scattering data from Ref. [1] in a single figure

TABLE I. Optical potentials for $p + {}^4\text{He}$ and $p + t$. Volume terms are denoted for the real part with a V subscript and with a W subscript for the imaginary term, while surface terms are denoted with an S subscript. Additional small spin-orbit terms were necessary to fit the data. However because in FRESKO it was not possible to introduce such terms, instead a proton spin-orbit potential of Thomas form with parameters $V_{so} = 9.96$ MeV, $r_{so} = 1.35$ fm, and $\alpha_{so} = 0.69$ fm was added to the diagonal ${}^7\text{Li} + p$ Watanabe folding potentials.

E (MeV/u)	System	V (MeV)	R_V (fm)	α_V (fm)	W (MeV)	R_W (fm)	α_W (fm)	W_S (MeV)	R_{WS} (fm)	α_{WS} (fm)
2.29	$p-t$	41.283	1.577	0.69	0.4	1.498	0.69	1.08	1.498	0.69
3.57	$p-t$	32.813	1.577	0.69	0.1	1.498	0.69	1.08	1.498	0.69
5.00	$p-t$	31.314	1.577	0.69	1.360	1.498	0.69	1.08	1.498	0.69
5.44	$p-t$	29.983	1.577	0.69	1.340	1.498	0.69	1.08	1.498	0.69
2.29	$p-{}^4\text{He}$	59.226	1.100	0.477	0.041	1.100	0.477			
3.57	$p-{}^4\text{He}$	54.226	1.100	0.477	0.041	1.100	0.477			
5.00	$p-{}^4\text{He}$	48.949	1.100	0.477	0.041	1.100	0.477			
5.44	$p-{}^4\text{He}$	51.226	1.100	0.477	0.041	1.100	0.477			

(Fig. 5). A similar plot of the inelastic scattering to the 0.478 MeV $1/2^-$ state of ${}^7\text{Li}$ is given as Fig. 7 of Ref. [1]. The calculations provide good descriptions of the elastic scattering and reasonable descriptions of the inelastic scattering data at all the energies, the data at 2.29 MeV/u being satisfactorily described by a two-channel calculation including just ground state reorientation and excitation of the bound $1/2^-$ excited state of ${}^7\text{Li}$ while the other energies require the inclusion of couplings to the continuum for the best description, as described above.

The elastic scattering data at 5.44 MeV/u are presented in more detail in Fig. 6 and compared with existing data at 6.1 MeV/u [6] as well as the results of various calculations. We can see that the one-channel and two-channel calculations,

the latter almost identical to the first, deviate significantly from the data. Switching on the direct coupling to the nonresonant continuum the agreement with the data slightly improves at forward angles only. Finally, switching on both direct and sequential breakup coupling via the 4.63 MeV resonance (2.163 MeV above the breakup threshold), the agreement between the calculation and the data is excellent. As noted in Ref. [3], the resonant coupling proves to have the strongest effect on the elastic scattering although the sequential breakup cross section is only 0.52 mb versus a total breakup cross section of 66 mb (see Table II). We show this explicitly in Fig. 6 by plotting the result of the calculation omitting the coupling to the resonance (the cyan curve), which was not done in Fig. 1 of Ref. [3].

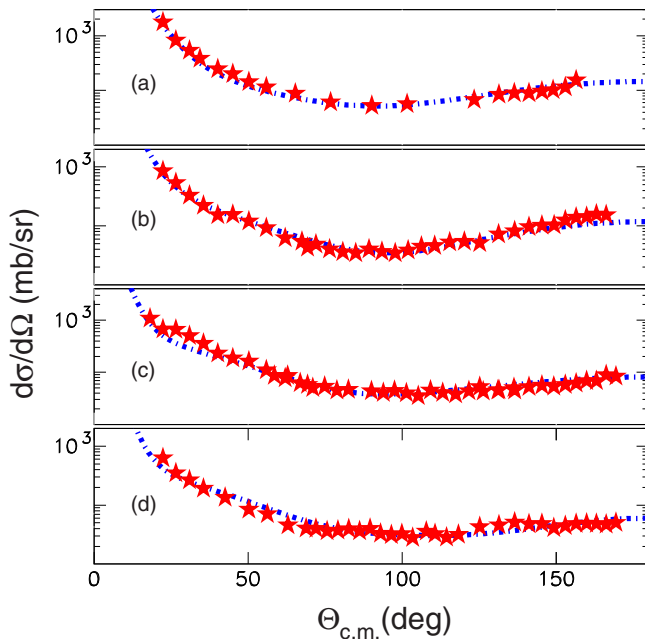


FIG. 5. Elastic scattering angular distributions for ${}^7\text{Li} + p$ at (a) 2.29 MeV/u, (b) 3.57 MeV/u, (c) 5.00 MeV/u, and (d) 5.44 MeV/u. FRESKO calculations are also shown as the dot-dashed blue lines, one-channel for panel (a) and full CDCC for panels (b), (c), and (d). Details of the measurement and calculations are also reported in Ref. [1].

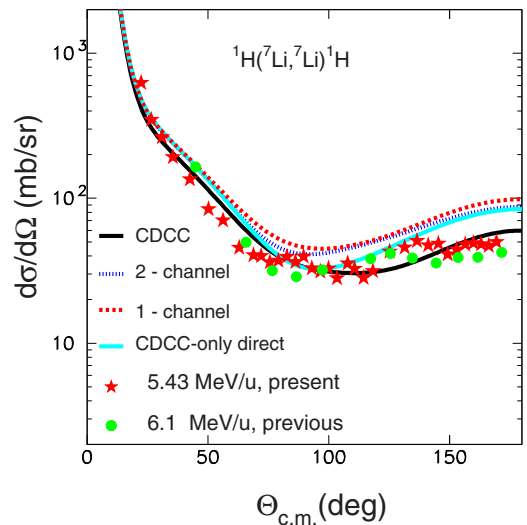


FIG. 6. The elastic scattering angular distribution at 5.44 MeV/u (red stars) compared with previous data at 6.1 MeV/u (green circles) [6] and the following FRESKO calculations: one-channel (dashed red line), two-channel (dotted blue line), full CDCC (solid black line), and finally a CDCC calculation omitting coupling to the resonance (solid cyan line). It is obvious that at backward angles the effect of coupling to the resonance is very strong. This figure is based on Fig. 4 of Ref. [1] and Fig. 1 of Ref. [3], including additional calculations via decoupling of resonance and direct breakup.

TABLE II. Experimental and theoretical cross sections for all open channels in the ${}^7\text{Li} + p$ system at 5.44 MeV/u, namely inelastic scattering, charge exchange, the ${}^7\text{Li} + p \rightarrow {}^4\text{He} + {}^4\text{He}$ reaction, and breakup. The cross section of 500 mb in the third column is the CDCC prediction for absorption out of the elastic channel, excluding inelastic scattering and breakup, and corresponds to the sum of the experimental cross sections for the charge exchange and (p, α) reactions, i.e., $\sigma_{\text{absorption}} = 361 \pm 39 + 61 \pm 10 + 27 \pm 3 = 449 \pm 40$ mb. The total reaction cross section resulting from this experiment is $\sigma_{\text{tot}} = 587$ mb compared with the theoretical value given by our CDCC calculation of $\sigma_{\text{tot}}^{\text{theo}} = 722$ mb. The difference between these two values ($722 - 587 = 135$ mb) is accounted for by the reorientation effect, which cannot be determined experimentally.

Reaction	σ_{exp} (mb)	σ_{CDCC} (mb)
${}^7\text{Li} + p \rightarrow {}^7\text{Li}^* + p$	65 ± 12	47
${}^7\text{Li} + p \rightarrow {}^7\text{Be} + n$	361 ± 39	} 500
${}^7\text{Li} + p \rightarrow {}^7\text{Be}^* + n$	61 ± 10	
${}^7\text{Li} + p \rightarrow {}^4\text{He} + {}^4\text{He}$	27 ± 3	
${}^7\text{Li} + p \rightarrow {}^4\text{He} + {}^3\text{H} + p$	72 ± 11	66

In addition to the elastic and inelastic scattering angular distributions FRESKO also provides angular distributions for the ${}^7\text{Li} \rightarrow \alpha + t$ breakup. An exclusive breakup measurement was performed at 5.44 MeV/u, simultaneously with elastic scattering, charge exchange, and the reaction leading to two α 's, by detecting the α particle fragment in the MAGNEX spectrometer in coincidence with the triton fragment in a silicon detector installed at 5° . Details of the data reduction may be found in Ref. [3], where an interesting point which we wish to emphasize here is the ‘‘philosophy’’ behind the Monte Carlo program. This was developed [13] to determine the efficiency of the MAGNEX spectrometer coupled to the 5° silicon detector and was based on the energy discretization of the continuum in the CDCC approach. The excellent agreement, outlined in Ref. [3], between experiment and the simulation based on the CDCC calculation, reinforces the realism of the philosophy behind the CDCC approach and vice versa.

Finally, the FRESKO calculations provide an absorption cross section that accounts for all other reaction channels not included explicitly in the calculation. We have already demonstrated that the CDCC calculations describe well the elastic and inelastic scattering and, at 5.44 MeV/u, the breakup (see Fig. 6, Fig. 7 of Ref. [1], and Fig. 5 of Ref. [3]). Because at this energy the only other open reaction channels are the ${}^7\text{Li} + p \rightarrow {}^7\text{Be} + n$ charge exchange and ${}^7\text{Li} + p \rightarrow {}^4\text{He} + {}^4\text{He}$ reactions it should follow that the absorption cross section given by FRESKO equals the sum of the experimental cross sections for the ${}^7\text{Li} + p \rightarrow {}^7\text{Be} + n$ charge exchange and the ${}^7\text{Li} + p \rightarrow {}^4\text{He} + {}^4\text{He}$ reactions. Table II shows that this is indeed the case to better than 10%.

In Fig. 7 we compile available data for the ${}^7\text{Li}(p, p')$ inelastic scattering, the ${}^7\text{Li}(p, n)$ charge exchange, and ${}^7\text{Li}(p, \alpha)$ reactions together with the results of our CDCC calculations over the energy range investigated here. The absorption cross sections from the CDCC calculations show good consistency with the sum of the ${}^7\text{Li}(p, n)$ charge exchange and ${}^7\text{Li}(p, \alpha)$

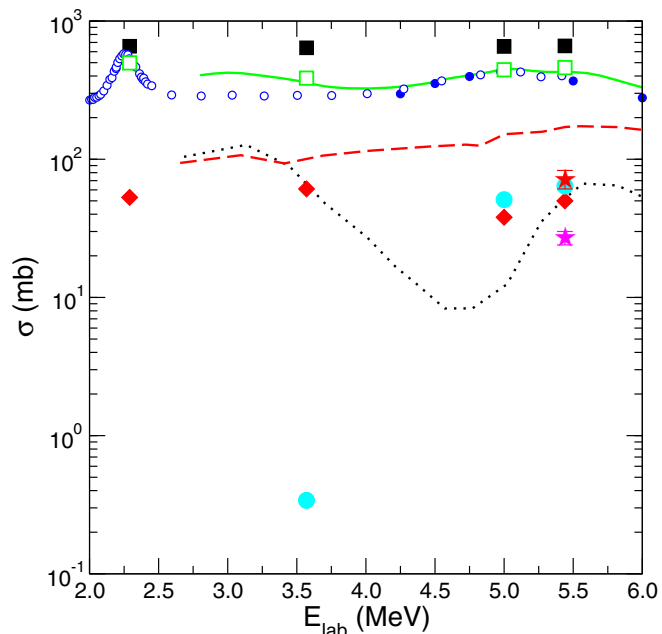


FIG. 7. Comparison of existing data for the ${}^7\text{Li} + p$ system with the results of CDCC calculations fitting measured elastic scattering. The dotted black and dashed red curves denote the ${}^7\text{Li}(p, \alpha)$ and ${}^7\text{Li}(p, p')$ inelastic scattering excitation functions of Ref. [6], respectively. The small solid and open blue circles denote the total (ground plus first excited state of ${}^7\text{Be}$) charge exchange excitation functions of Refs. [4] and [14], respectively, validated by the present data. The solid green curve denotes the sum of the interpolated charge exchange and ${}^7\text{Li}(p, \alpha)$ excitation functions. The large solid cyan circles denote the calculated total breakup cross sections, the large solid red diamonds the calculated ${}^7\text{Li}(p, p')$ inelastic scattering cross sections, the large open green squares the calculated total absorption cross sections, and the large solid black squares the calculated total reaction cross sections. The datum denoted with a red star (the upper star) refers to our breakup measurement reported in Ref. [3] and obtained at an experiment simultaneously with the data reported here. Also the datum denoted with the magenta star (the lower star) refers to the present measurement of the reaction ${}^7\text{Li} + p \rightarrow {}^4\text{He} + {}^4\text{He}$.

reactions at all energies while the inelastic scattering cross sections of Ref. [6] are consistently underpredicted. This is in part due to a poor representation of the shape of the inelastic scattering angular distributions at large scattering angles—the calculations drop rapidly whereas the data are relatively ‘‘flat’’ as a function of angle—but the absolute normalization of the data of Ref. [6] also tends to be somewhat larger than the present measurement.

It is apparent from Fig. 7 that the total reaction cross section is dominated by the charge exchange contribution, breakup hardly contributing in this energy range due to the proximity of the threshold for this reaction (cf. the rapid rise of the total breakup cross section as the incident proton energy increases from 3.5 MeV). It is also apparent that despite the presence of resonances in both the charge exchange and ${}^7\text{Li}(p, \alpha)$ reactions these are not manifest in the total reaction cross section, which remains relatively constant over this energy range, a reflection of the measured elastic scattering angular distributions that

also show no sign of any resonance behavior, varying smoothly with incident proton energy. Resonances in the exit channels therefore do not appear to have significant impact on the elastic scattering, providing *a posteriori* justification for the use of CDCC to analyze these low-energy data.

IV. SUMMARY AND CONCLUSIONS

A global study of the ${}^7\text{Li} + p$ system at 5.44 MeV/u was carried out considering all open reaction channels, namely elastic scattering, inelastic scattering, breakup, the charge exchange populating the ground and first excited states of ${}^7\text{Be}$, and the transfer/compound reaction leading to two α particles in the exit channel. Since all the reactions were measured in the same experiment the overall normalizations should be reliable. The charge exchange was observed to be by far the most populated channel at this rather low incident energy.

A CDCC calculation taking into account the cluster structure of the weakly bound projectile was performed using the FRESKO code. Comparisons with the experimental angular distributions for elastic scattering and breakup gave strong evidence for the important influence on the elastic scattering of coupling to sequential breakup at this energy, despite the predicted very low cross section compared to the direct, nonresonant breakup. Due to the small number of open channels at this energy the absorption cross section obtained

from the FRESKO calculation may be equated to the sum of the charge exchange and (p, α) reaction cross sections. An inspection of Table II shows that the theoretical breakup cross section agrees, within errors, with the experimental one while the CDCC absorption cross section, $\sigma_{\text{abs}} = 500$ mb, agrees with the sum of the experimental charge exchange and (p, α) cross sections, $\sigma_{\text{exp}} = (361 \pm 39) + (61 \pm 10) + (27 \pm 3) = 449 \pm 40$ mb to better than 10%. The calculated inelastic cross section (to the 0.478 MeV $1/2^-$ state) deviates by about 40% from the measured one but our angular distribution was obtained over a very narrow angular range so the comparison may be misleading. The inelastic cross section of Ref. [6] is rather larger at this energy but is again the result of a Legendre polynomial fit to relatively limited data.

By interpolating existing reaction measurements we also demonstrated that CDCC calculations at 2.29, 3.57, and 5.0 MeV/u gave absorption cross sections that were consistent with the sum of the charge exchange and (p, α) reaction cross sections. Overall we conclude that the new data for the charge exchange reaction validate the normalization of Refs. [4,5,14] while the new (p, α) data yield an integrated cross section about 3/5 that of the interpolated previous data of Ref. [6]. Taken together, the available data further validate the CDCC theoretical approach to the description of the ${}^7\text{Li} + p$ system at these low energies in a global context since the presence of resonant behavior in the exit channels does not appear to manifest in the elastic scattering or total reaction cross sections.

-
- [1] A. Pakou, V. Soukeras, F. Cappuzzello *et al.*, *Phys. Rev. C* **94**, 014604 (2016).
 - [2] F. Cappuzzello, C. Agodi, D. Carbone, and M. Cavallaro, *Eur. Phys. J. A* **52**, 167 (2016).
 - [3] A. Pakou, O. Sgouros, V. Soukeras, F. Cappuzzello *et al.*, *Phys. Rev. C* **95**, 044615 (2017).
 - [4] C. H. Poppe, J. D. Anderson, J. C. Davis, S. M. Grimes, and C. Wong, *Phys. Rev. C* **14**, 438 (1976).
 - [5] C. A. Burke, M. T. Lunnion, and H. W. Lefevre, *Phys. Rev. C* **10**, 1299 (1974).
 - [6] K. Kilian, G. Clausnitzer, W. Dürr, D. Fick, R. Fleischmann, and H. M. Hofmann, *Nucl. Phys. A* **126**, 529 (1969).
 - [7] G. Marquín-Durán, L. Acosta, R. Berjillos *et al.*, *Nucl. Instrum. Methods Phys. Res., Sect. A* **755**, 69 (2014).
 - [8] I. J. Thompson, *Comput. Phys. Rep.* **7**, 167 (1988).
 - [9] G. Freier, E. Lampi, W. Sleator, and J. H. Williams, *Phys. Rev.* **75**, 1345 (1949).
 - [10] P. D. Miller and G. C. Phillips, *Phys. Rev.* **112**, 2043 (1958).
 - [11] J. E. Brolley, Jr., T. M. Putnam, L. Rosen, and L. Stewart, *Phys. Rev.* **117**, 1307 (1960).
 - [12] R. Kankowsky, J. C. Fritz, K. Kilian, A. Neufert, and D. Fick, *Nucl. Phys. A* **263**, 29 (1976).
 - [13] O. Sgouros, V. Soukeras, and A. Pakou, *Eur. Phys. J. A* **53**, 165 (2017).
 - [14] J. H. Gibbons and R. L. Macklin, *Phys. Rev.* **114**, 571 (1959).